PCCP

Cite this: *Phys. Chem. Chem. Phys.*, 2011, **13**, 16861–16866

www.rsc.org/pccp

PAPER

Aromaticity of strongly bent benzene rings: persistence of a diatropic ring current and its shielding cone in [5]paracyclophane†

Leonardus W. Jenneskens,*[a] Remco W. A. Havenith,[b] Alessandro Soncini[c] and Patrick W. Fowler*[d]

Received 15th June 2011, Accepted 3rd August 2011
DOI: 10.1039/c1cp21950b

Direct evaluation of the induced π current density in [5]paracyclophane (**1**) shows that, despite the significant non-planarity (α = 23.2°) enforced by the pentamethylene bridge, there is only a modest (*ca.* 17%) reduction in the π ring current, justifying the use of shielding-cone arguments for the assignment of ^{1}H NMR chemical shifts of **1** and the claim that the non-planar benzene ring in **1** retains its aromaticity (on the magnetic criterion).

Introduction

Some compounds for which the question of aromaticity is of particular interest are the short-bridged [*n*]para- and [*n*]meta-cyclophanes, where the natural aromaticity of the benzene ring is placed under attack by the bending enforced by the bridge.[1,2] An influential school of thought considers aromaticity to be *defined* by the existence of a diatropic ring current[2,3] and hence, operationally, that the persistence of aromaticity in bridged molecules such as [5]- and [6]paracyclophane[1,4] can be inferred from consistency of ^{1}H chemical shifts with a ring-current model. With the advent of efficient methods for computation and visualisation of induced current density,[5] it has become possible to explore the putative aromaticity of molecules such as cyclophanes by direct calculation. The calculations reported here show that [5]paracyclophane (**1**)[1] supports a diatropic ring current that is diminished by only *ca.* 17% with respect to that of planar D_{6h} benzene and arises from the descendants of the orbitals involved in the same characteristic frontier electronic structure in benzene. Analysis of the corresponding shielding-density maps explains the 'shielding-cone' effects on ^{1}H chemical shifts that were used to identify this molecule on its first synthesis.[1] For comparison, properties were also calculated in the present study for a valence isomer of **1**, *i.e.*, 1,4-pentamethylene Dewar benzene (**2**).[6]

Computational details

Geometries of **1** and **2** were optimised at the RHF/6-31G** level using GAMESS-UK.[7] Current-density and shielding-density maps for **1** and **2** were computed, using SYSMO,[8] at the 'ipsocentric' CTOCD-*DZ*/6-31G**//RHF/6-31G** level, the specific conceptual and practical advantages of which have been rehearsed elsewhere.[5c,3g] An important advantage of the distribution of origin over the whole of molecular space is that a relatively modest basis set is then sufficient to give maps that are close to (in this case) the Hartree–Fock limit, at much reduced cost, and avoiding the artefacts associated with single-origin calculations in unsaturated basis sets.[9] In addition, here we have exploited the ability of the ipsocentric approach to provide additive, physically non-redundant, orbital contributions to current density, and so to identify the 'π' ring current (if any) arising from the descendants of the benzene π orbitals in [5]paracyclophane (**1**). ^{1}H shielding tensors and chemical shifts were computed using a distributed-origin method: the CTOCD-*PZ*2 variant[10] of the ipsocentric approach, again using SYSMO.[8]

Results and discussion

(i) Optimised structures of 1 and 2

The RHF/6-31G** optimised structures of [5]paracyclophane (**1**) and its valence isomer 1,4-pentamethylene Dewar benzene (**2**) are shown in Fig. 1 (see also ESI, Tables S1 and S2).†

Both **1** and **2** adopt C_s geometries, with 8 symmetry-distinct ^{1}H sites (numbered as in Fig. 1), in agreement with available experimental NMR data[1,6] and with earlier computational results.[11] In short, although **1** possesses a markedly non-planar benzenoid ring [Fig. 1: α = 23.2° (*cf.* STO-3G 22.4°,

[a] *Organic Chemistry & Catalysis, Debye Institute for Nanomaterials Science, Utrecht University, Universiteitsweg 99, 3584 CG Utrecht, Netherlands. E-mail: l.w.jenneskens@uu.nl; Fax: +31-30-2523615; Tel: +31-30-2533128*
[b] *Theoretical Chemistry, Zernike Institute for Advanced Materials, University of Groningen, Nijenborgh 4, 9747 AG Groningen, Netherlands. E-mail: r.w.a.havenith@rug.nl*
[c] *School of Chemistry, University of Melbourne, Victoria 3010, Australia. E-mail: asoncini@unimelb.edu.au*
[d] *Department of Chemistry, University of Sheffield, Sheffield S3 7HF, UK. E-mail: P.W.Fowler@sheffield.ac.uk*

† Electronic supplementary information (ESI) available: RHF/6-31G** (Tables S1–S2) and Fig. S1 for **1** and **2** and CTOCD-*DZ*/6-31G**//RHF/6-31G** data (Fig. S2) for **2**. See DOI: 10.1039/c1cp21950b

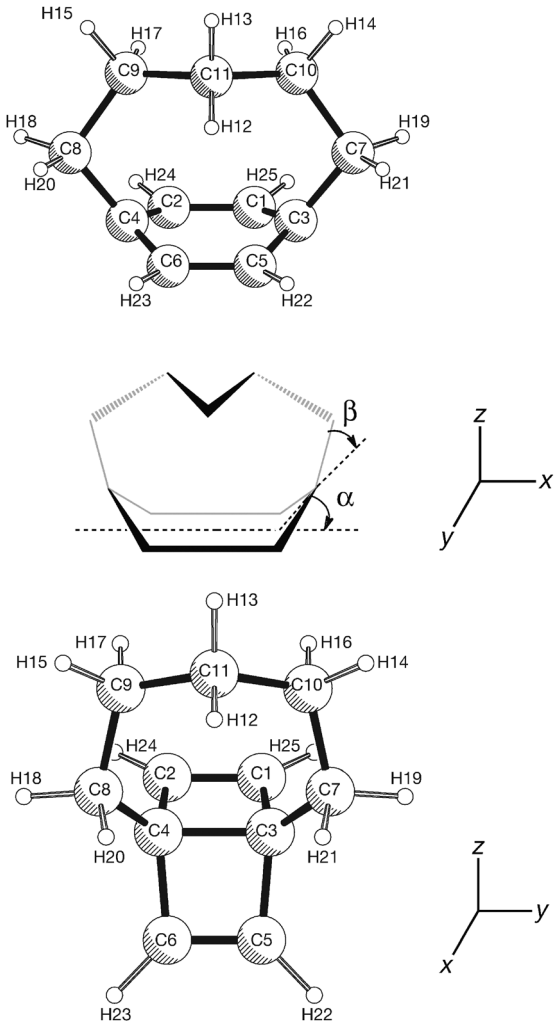

Fig. 1 RHF/6-31G** geometries of **1**, C_s (top) and **2**, C_s (bottom), with atom numbering and (middle) projected angles for **1**, $\alpha = 23.2^\circ$ and $\beta = 29.5^\circ$.

DZ 23.7°,[11a] 6-31 G 23.5°,[11b] DZP 23.5°[11c]) and $\beta = 29.5^\circ$ (DZP 28.7°[11c])], its carbon–carbon lengths [mean value 1.388 Å (see ESI†, Fig. S1)] fall in the usual range for planar D_{6h} benzene at the RHF/6-31G** level of theory. As expected,[1,6,11] **2** contains two typical olefinic bonds [1.321 Å, see ESI†, Fig. S1 (*cf.* 6-31G 1.330 Å)[11b]]. We note that the geometric parameters, and in particular the angles, are relatively insensitive to the size of the basis set employed, as the above comparisons show. In the adopted Cartesian coordinate system, which is the principal inertial frame of the ^{12}C, ^{1}H isotopomer, the z direction runs from the six-membered ring towards the saturated alkane-bridge for both **1** and **2**. The reference plane for the calculation of π current in planar D_{6h} benzene is the plane of the nuclei: induced current is calculated at a height of $1a_0$ (0.529 Å) above this plane, where the charge and current densities arising from the occupied p_π orbitals are both expected to be close to maximal. Other techniques, such as those based on NICS (Nucleus Independent Chemical Shifts)[3f] and measures derived from them,[12] often take the reference height as 1 Å. This greater distance from the molecular plane is needed there to combat the problem of σ/π contamination, which cannot be entirely excluded in NICS calculations.[13] In the present case, the ipsocentric approach allows a clean separation of the contributions of occupied π orbitals from the rest, and the height can be chosen to be optimal for the p_π orbitals.

(ii) Persistence of a diatropic ring current in 1

In the present case, the reference (zero) plane for **1** and **2** is chosen parallel to the xy inertial plane and passes close to the four central carbon atoms of the six-membered ring (**1**, Fig. 1: C_1, C_2, C_5 and C_6), with two (C_1 and C_2) of the four at $z = +0.082a_0$ and two (C_5 and C_6) at $z = -0.082a_0$. Currents were plotted (a) in this plane, and at $1a_0$ above and below. The plots in the reference plane were made in order to check the π-like character of any circulation, and the plots above and below were made in order to disentangle π-circulation from any effects arising from contributions of σ bonds crossing the plotting plane. Fig. 2 shows the resulting maps for the current arising in the three plotting planes when **1** is subjected to an external magnetic field directed along the z-axis. For each plane, two plots are made, one of the contribution from *all* [total (σ + π)] electrons (Fig. 2) and one of the contribution from the four π electrons of the HOMO and (HOMO − 1) pair (Fig. 3). Whereas in planar D_{6h} benzene itself the e_{1g} HOMO is doubly degenerate, in the lower symmetry of **1** (C_s) this pair splits to a'' (HOMO) + a' (HOMO − 1). The *para*-bridged benzene ring in **1** is non-planar[14,15] and the pair identified as the direct descendants of the benzene e_{1g} π HOMO are the HOMO ($17a''$) and HOMO − 1 ($23a'$) of **1**. That these molecular orbitals do indeed retain the essential nodal characteristics of their benzene ancestors can be seen from Fig. 4.

A number of previous studies have considered the influence of distortions of benzene on various aromaticity indices.[16] In general, indicators of aromaticity are found to be resilient under geometric distortion, and this is compatible with the idea that the nodal character of the frontier orbitals is slow to change, and that geometric distortion is more effective in reducing ring-current aromaticity when it is associated with a change in that character.[17]

A useful quantitative measure of the induced π ring current is j_{max}: the largest value over the plotting plane of the induced current density per unit inducing field. The standard for comparison is the value of $j_{max} = 0.080$ a.u.[18] for planar D_{6h} benzene, computed at a height of $1a_0$, within the same ipsocentric approach and using the same 6-31G** basis set.[18] For **1** the summed contributions of the HOMO ($17a''$) and HOMO-1 ($23a'$) give $j_{max} = 0.128$, 0.354, 0.066 a.u., respectively, in the $+1a_0$, 0, $-1a_0$ planes. Note that the large j_{max} values for the $+1a_0$ and 0 planes reflect strong highly localised currents near nuclei or cutting of σ-bonds by the plotting plane. This complication notwithstanding, the j_{max} value (0.066 a.u.) computed in the $-1a_0$ plane for the non-planar benzenoid ring of **1** signals the presence of a substantial diatropic π ring current of the classic benzenoid type; only a modest (*ca.* 17%) reduction is found when compared to planar D_{6h} benzene ($j_{max} = 0.080$ a.u.[18]).

Inspection of the maps, particularly those of the summed HOMO ($17a''$) + [HOMO − 1 ($23a'$)] contribution (Fig. 3),

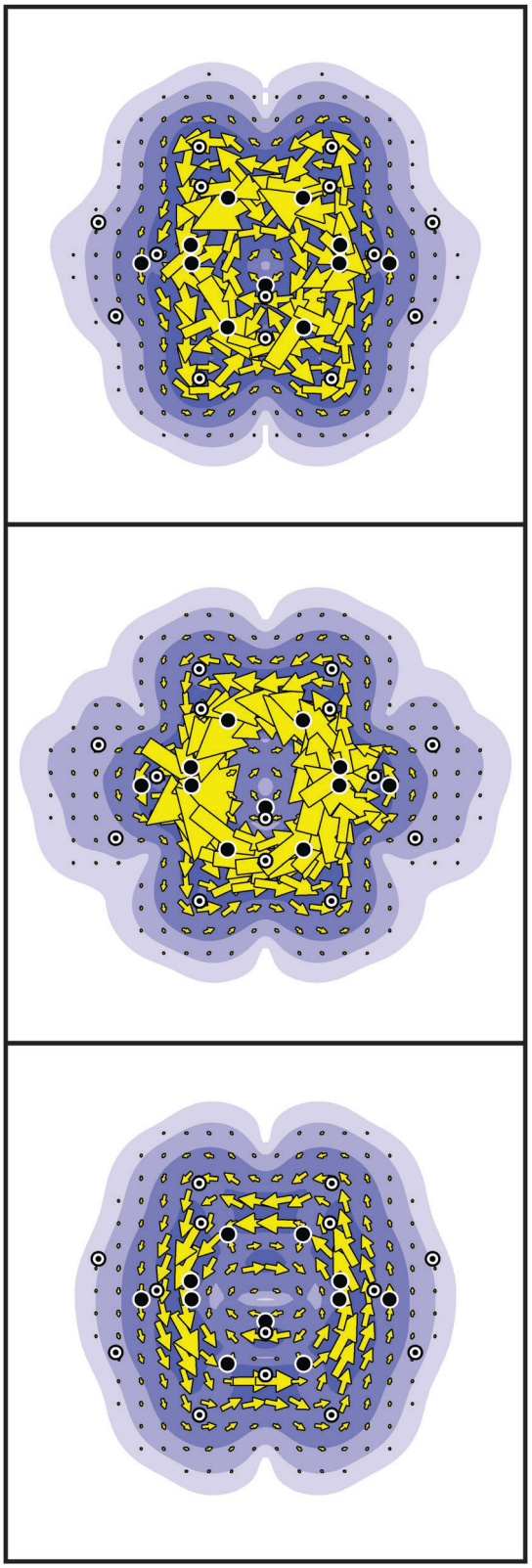

Fig. 2 CTOCD-*DZ*/6-31G**//RHF/6-31G** total (σ + π) current density maps of **1** (from top to bottom panels): in the reference (zero) plane, at $1a_0$ above and $1a_0$ below this plane. The usual plotting conventions apply: contours represent the modulus, and arrows the in-plane component of the current-density vector.[5c]

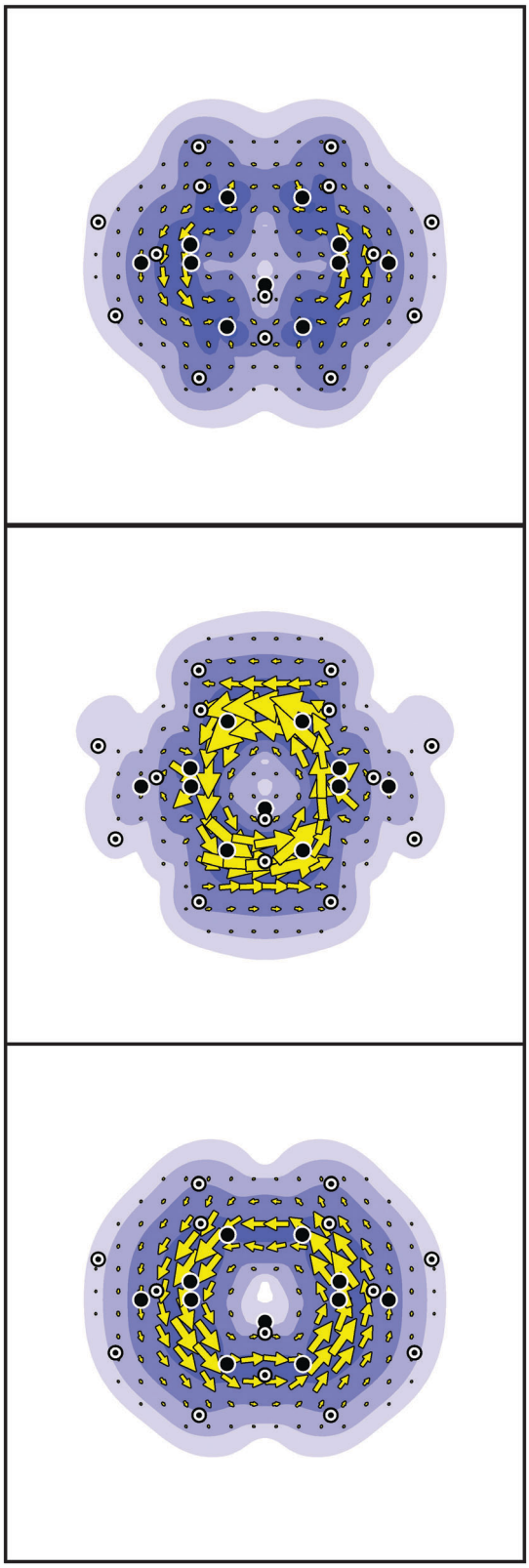

Fig. 3 CTOCD-*DZ*/6-31G**//RHF/6-31G** summed [HOMO ($17a''$) + (HOMO − 1 ($23a'$)] π current density maps of **1** (from top to bottom panels): in the reference (zero) plane, at $1a_0$ above and $1a_0$ below this plane. The usual plotting conventions apply: contours represent the modulus, and arrows the in-plane component of the current-density vector.[5c]

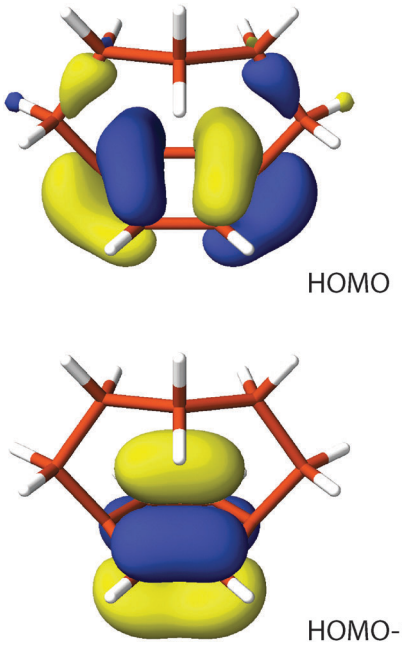

Fig. 4 RHF/6-31G** π-like molecular orbitals of [5]paracyclophane (**1**) [(top) HOMO ($17a''$) and (bottom) HOMO − 1 ($23a'$)].

reveals a simple message. The strongly bent benzene ring (α = 23.2°, Fig. 1) of **1** still sustains a *global* diamagnetic circulation that (i) is associated with the ring of six carbon sites (C_1–C_6, Fig. 1), (ii) is minimal near the zero plane, (iii) is roughly uniform in strength around the ring perimeter, and (iv) is dominated by the contributions of these two molecular orbitals. Four-electron diatropicity is a characteristic of aromatic $4n + 2\pi$-electron monocycles, with a simple rationalisation in terms of selection rules for diatropic and paratropic currents within the ipsocentric approach.[19] Thus, we can see that [5]paracyclophane (**1**) supports a diatropic π ring current that shares all the hallmarks of sense of circulation, spatial distribution and orbital origin with the classic current of undistorted D_{6h} benzene.

(iii) Shielding cone of [5]paracyclophane (1)

Effects on ^{1}H chemical shifts of benzenoid *vs.* aliphatic bridge hydrogens are fundamental to the verification of the ring-current model.[3c] They are embodied in shielding-density maps,[20] which give a classical interpretation of the *local* magnetic field at each point in molecular space, based on the idea that the Biot–Savart law[21] can be taken to apply in a differential form to each infinitesimal element of the quantum-mechanical current density. Each shielding-density map is in effect a different geometrically scaled version of the current-density map; integration of the maps within each plane and over all parallel planes retrieves a component of the nuclear shielding tensor σ.

In ref. 20*a* it was previously shown that a *global* ring current has a specific signature in the shielding-density map for the *out-of-plane* component of nuclear shielding at an *exo* ^{1}H site, the hydrogens of planar D_{6h} benzene. Such a map for an aromatic ring shows deshielding spike features close to the *exo* ^{1}H site itself, but a shielding ridge associated with the remote

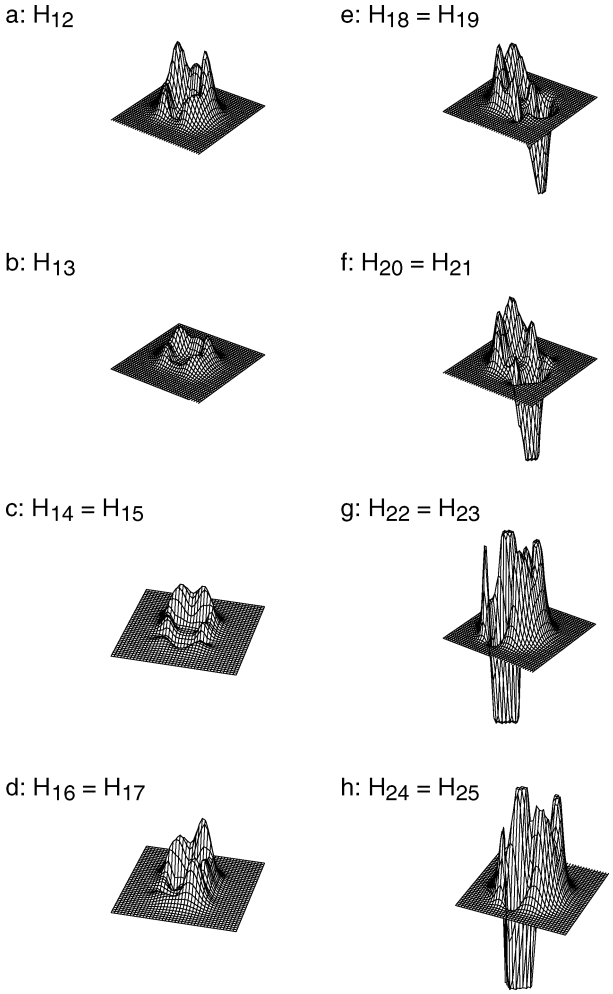

Fig. 5 Projections of shielding-density maps for eight symmetry-distinct ^{1}H nuclei of **1**, numbered as in Fig. 1. The maps are plotted in appropriate projections for the $-1a_0$ plane. They represent the contributions from the highest-lying pair [HOMO ($17a''$) + HOMO − 1 ($23a'$)] of π-like orbitals to the component of shielding, $\sigma_{\pi,zz}$(H), parallel to the external field.

portion of the ring of carbon atoms. It is the incomplete cancellation of these two features that differentiates *global* ring current from *local* bond currents. Fig. 5 shows shielding-density maps for each distinct ^{1}H site in **1**.

The main features of the maps are typically opposing trough/ridge and up/down-spike structures that can be clearly associated with the circuit of atoms, consistent with the existence of a ring current in the underlying global current-density map. The set of shielding densities give a clear indication of the effect of this ring current on each symmetry distinct ^{1}H sites (Fig. 1). In the adopted Cartesian coordinate system of **1** this will be reflected by $\sigma_{\pi,zz}$(H) contributions. Easiest to see is the shielding density at the distinct *exo* ^{1}H sites on the non-planar benzenoid six-membered ring [Fig. 5: (g) H_{22} = H_{23} and (h) H_{24} = H_{25}, *cf.* also Fig. 1]. In these cases, the maps present the classic signature of the *deshielding* effect of a benzene-like π ring-current on protons (*exo* ^{1}H sites) located outside the anisotropy cone:[22] each shows a low shielding ridge over the far side of the ring, outweighed by the local

deshielding spike associated with the nearby part of the ring. The integrated π contribution to the *zz* component, $\sigma_{\pi,zz}$(H), of the shielding tensor is strongly deshielding in these two cases. This contribution can be estimated by making approximate orbital decompositions of the results of CTOCD-*PZ*2 calculations of the ^{1}H nuclear magnetic shieldings σ in the same 6-31G** basis used to construct the maps. We find $\sigma_{\pi,zz}(H_{22}/H_{23}) = -1.66$ ppm and $\sigma_{\pi,zz}(H_{24}/H_{25}) = -2.02$ ppm (Fig. 5).

The (benzylic) ^{1}H sites attached to the first aliphatic carbons of the pentamethylene bridge [Fig. 5: (e) $H_{18} = H_{19}$ and (f) $H_{20} = H_{21}$, *cf*. also Fig. 1], as expected from their positions closer to the classical cone of anisotropy have a smaller overall ring-current response, shown by the reduced height variation in the maps. In fact, on integration, the π contribution to the *zz* component of the shielding tensor $\sigma_{\pi,zz}$ turns out to be already slightly *shielding* in these cases [Fig. 5: $\sigma_{\pi,zz}(H_{18}/H_{19}) = +0.58$ ppm and $\sigma_{\pi,zz}(H_{20}/H_{21}) = +0.34$ ppm].

Moving further into the bridge, the remaining symmetry distinct ^{1}H sites are all positioned *inside* the classic anisotropy cone, and the maps for these sites [Fig. 5: (a) H_{12}, (b) H_{13}, (c) $H_{14} = H_{15}$ and (d) $H_{16} = H_{17}$ (*cf*. also Fig. 1)] all show an increasing effect of the shielding ridge. The deshielding spike becomes more localised and less intense [Fig. 5: (a), (c) and (d)], and indeed vanishes altogether for H_{13} [Fig. 5(b)]. In all four cases, the integrated π contribution, $\sigma_{\pi,zz}$(H), turns out to be a net *shielding* and is larger for the ^{1}H sites closer to the six-membered ring [Fig. 5: $\sigma_{\pi,zz}(H_{12}) = +2.86$ ppm; $\sigma_{\pi,zz}(H_{13}) = +1.14$ ppm; $\sigma_{\pi,zz}(H_{14}) = +1.45$ ppm; $\sigma_{\pi,zz}(H_{16}/H_{17}) = +1.71$ ppm].

The shielding ridge in the map for H_{13} represents a complete circuit, imaging the π ring current, and in this particularly simple case can be recognised as exactly the situation implied in the NICS[3f,12] concept: H_{13} could be considered to act as a probe, dangled into the central part of the shielding cone. Evaluation of its ^{1}H chemical shift at a test point in similar relation to a benzene ring would give a negative value, which, would then, correctly in this case, be interpretable as evidence for a diatropic ring current.

(iv) 1,4-Pentamethylene Dewar benzene (2)

For completeness, ring-current and shielding-density maps were also computed for **2**. As might be expected, this bridged Dewar benzene shows no evidence of any global ring current. The current-density maps show only localised circulations associated with the two formal double bonds (C_1–C_2 and C_5–C_6) of the bent six-membered ring (see ESI†, Fig. S2), and the shielding-density maps all show the localised and near-cancelling up- and down-spikes characteristic of localised currents in the carbon–hydrogen bond, rather than the remote trough/ridge features that would indicate the presence of a global ring current. In view of their lack of information in the context of aromaticity, these maps are not shown here.

Conclusions

Here we have shown that, on the magnetic criterion, the benzene ring of [5]paracyclophane (**1**) is aromatic in that it supports a substantial diatropic π ring current with the same orbital origin as in planar D_{6h} benzene itself, strain and non-planarity notwithstanding. Only a minor (*ca*. 17%) reduction of the π ring current is found (*cf*. also ref. 2).

In their computational study of the energetics and properties of the lower homologue of [5]paracyclophane (**1**), *viz*. [4]paracyclophane, Ma *et al*.[23] have reviewed the arguments that have been used for and against the attribution of aromaticity to the benzene ring of [5]paracyclophane (**1**).[11a,23] Said to count against aromaticity are: the different reactivity of **1** and benzene, the non-planarity of the benzenoid ring, and the high strain energy of **1**. Said to count for aromaticity are: the similarities in vibrational frequencies between **1** and *p*-dideuteriobenzene, the low degree of bond alternation in the benzene ring of **1**,[11a,23] its UV/Vis characteristics and ^{1}H NMR properties.[1,2,11,15,16,23] Our study has confirmed in detail that the magnetic properties stem from an underlying 'aromatic' ring current, as in benzene itself.

Notes and references

1 L. W. Jenneskens, F. J. J. De Kanter, P. A. Kraakman, L. A. M. Turkenburg, W. E. Koolhaas, W. H. de Wolf, F. Bickelhaupt, Y. Tobe, K. Kakiuchi and Y. Odaira, *J. Am. Chem. Soc*., 1985, **107**, 3716–3717.

2 P. C. M. van Zijl, L. W. Jenneskens, E. W. Bastiaan, C. MacLean, W. H. de Wolf and F. Bickelhaupt, *J. Am. Chem. Soc*., 1986, **108**, 1415–1418; see also L. W. Jenneskens, J. N. Louwen and F. Bickelhaupt, *J. Chem. Soc., Perkin Trans. 2*, 1989, 1893–1895.

3 (*a*) F. London, *J. Phys. Radium*, 1937, **8**, 397–409; (*b*) L. Pauling, *J. Chem. Phys*., 1936, **4**, 673–677; (*c*) J. A. Pople, *J. Chem. Phys*., 1956, **24**, 1111; (*d*) J. A. Elvidge and L. M. Jackman, *J. Chem. Soc*., 1961, 859–866; (*e*) H. J. Dauben, J. D. Wilson and J. L. Laity, *Nonbenzenoid aromatics*, ed. J. P. Snijder, Academic Press, New York, 1971, vol. II, pp. 167–206; (*f*) P. v. R. Schleyer, C. Maerker, A. Dransfeld, H. Jiao and N. J. R. van Eikema Hommes, *J. Am. Chem. Soc*., 1996, **118**, 6317–6318; (*g*) P. W. Fowler, E. Steiner, R. W. A. Havenith and L. W. Jenneskens, *Magn. Reson. Chem*., 2004, **42**, S68–S78.

4 For a review: V. V. Kane, W. H. de Wolf and F. Bickelhaupt, *Tetrahedron*, 1994, **50**, 4575–4622.

5 (*a*) T. A. Keith and R. F. W. Bader, *Chem. Phys. Lett*., 1993, **210**, 223–231; (*b*) P. Lazzeretti, M. Malagoli and R. Zanasi, *Chem. Phys. Lett*., 1994, **200**, 299–304; (*c*) P. W. Fowler and E. Steiner, *J. Phys. Chem*., 1997, **101**, 1409–1413.

6 J. W. van Straten, L. A. M. Turkenburg, W. H. de Wolf and F. Bickelhaupt, *Recl. Trav. Chim. Pays-Bas*, 1985, **104**, 89–97.

7 M. F. Guest, I. J. Bush, H. J. J. van Dam, P. Sherwood, J. M. H. Thomas, J. H. van Lenthe, R. W. A. Havenith and J. Kendrick, *Mol. Phys*., 2005, **103**, 719–747.

8 P. Lazzeretti and R. Zanasi, SYSMO package, University of Modena, 1980. Additional routines for the evaluation and plotting of current density: E. Steiner, P. W. Fowler, R. W. A. Havenith and A. Soncini.

9 P. W. Fowler, E. Steiner, R. Zanasi and B. Cadioli, *Mol. Phys*., 1999, **96**, 1099–1108.

10 R. Zanasi, *J. Chem. Phys*., 1996, **105**, 1460–1469.

11 (*a*) J. E. Rice, T. J. Lee, R. B. Remington, W. D. Allen, D. A. Clabo, Jr and H. F. Schaefer, III, *J. Am. Chem. Soc*., 1987, **109**, 2902–2909 and references cited; (*b*) M. von Arnim and S. D. Peyerimhoff, *Theor. Chim. Acta*, 1993, **85**, 43–59; (*c*) S. Grimme, *J. Am. Chem. Soc*., 1992, **114**, 10542–10547; see also: (*d*) P. v. R. Schleyer and F. Pühlhofer, *Org. Lett*., 2002, **4**, 2873–2876.

12 H. Fallah-Bagher-Shaidaei, C. S. Wannere, C. Corminboeuf, R. Puchta and P. v. R. Schleyer, *Org. Lett*., 2006, **8**, 863–866.

13 E. Steiner and P. W. Fowler, *Phys. Chem. Chem. Phys*., 2004, **6**, 261–272.

14 (*a*) H. Schmidt, A. Schweig, W. Thiel and M. Jones, Jr., *Chem. Ber*., 1978, **111**, 1958–1961; (*b*) R. Gleiter, H. Hopf, M. Eckert-Maksic and K. L. Noble, *Chem. Ber*., 1980, **113**, 3401–3403.

15 L. W. Jenneskens, E. N. van Eenige and J. N. Louwen, *New J. Chem.*, 1992, **16**, 775–779.
16 See also: (*a*) M. K. Cyrański and T. M. Krygowski, *Tetrahedron*, 1999, **55**, 6205–6210; (*b*) F. Dijkstra and J. H. van Lenthe, *Int. J. Quantum Chem.*, 1999, **74**, 213–221; (*c*) G. J. Bodwell, J. N. Bridson, M. K. Cyrański, J. W. J. Kennedy, T. M. Krygowski, M. R. Mannion and D. O. Miller, *J. Org. Chem.*, 2003, **68**, 2089–2098; (*d*) F. Feixas, E. Matito, J. Poater and M. Solà, *J. Phys. Chem. A*, 2007, **111**, 4513–4521.
17 A. Soncini, R. W. A. Havenith, P. W. Fowler, L. W. Jenneskens and E. Steiner, *J. Org. Chem.*, 2002, **67**, 4753–4758.
18 E. Steiner and P. W. Fowler, *Int. J. Quantum Chem.*, 1996, **60**, 609–616.
19 E. Steiner and P. W. Fowler, *Chem. Commun.*, 2001, 2220–2221; E. Steiner and P. W. Fowler, *J. Phys. Chem. A*, 2001, **105**, 9553–9562.
20 (*a*) A. Soncini, P. W. Fowler, P. Lazzeretti and R. Zanasi, *Chem. Phys. Lett.*, 2005, **401**, 164–169; see also: (*b*) S. Pelloni, A. Ligabue and P. Lazzeretti, *Org. Lett.*, 2004, **6**, 4451–4454.
21 J. D. Jackson, *Classical Electrodynamics*, John Wiley & Sons, New York, 3rd edn, 1999.
22 C. W. Haigh and R. B. Mallion, *Org. Magn. Reson.*, 1972, **4**, 203–228.
23 B. Ma, H. M. Sulzbach, R. B. Remington and H. F. Schaefer III, *J. Am. Chem. Soc.*, 1995, **117**, 8392–8400 and references cited.

